

Are “Generalized” Seizures Truly Generalized? Evidence of Localized Mesial Frontal and Frontopolar Discharges in Absence

*Mark D. Holmes, †Micah Brown, and ††Don M. Tucker

*Regional Epilepsy Center, Department of Neurology, University of Washington, Seattle, Washington; and †Electrical Geodesics, Inc., and ††Department of Psychology, University of Oregon, Eugene, Oregon, U.S.A.

Summary: *Purpose:* To determine whether specific regions of cerebral cortex are activated at the onset and during the propagation of absence seizures.

Methods: Twenty-five absence seizures were recorded in five subjects (all women; age 19–58 years) with primary generalized epilepsy. To improve spatial resolution, all studies were performed with dense-array, 256-channel scalp EEG. Source analysis was conducted with equivalent dipole (BESA) and smoothed linear inverse (LORETA) methods. Analyses were applied to the spike components of each spike–wave burst in each seizure, with sources visualized with standard brain models.

Results: For each patient, the major findings were apparent on inspection of the scalp EEG maps and waveforms, and the two methods of source analysis gave generally convergent results. The onset of seizures was typically associated with activation of discrete, often unilateral areas of dorsolateral frontal or orbital

frontal lobe. Consistently across all seizures, the negative slow wave was maximal over frontal cortex, and the spike that appeared to follow the slow wave was highly localized over frontopolar regions of orbital frontal lobe. In addition, sources in dorsomedial frontal cortex were engaged for each spike–wave cycle. Although each patient showed unique features, the absence seizures of all patients showed rapid, stereotyped evolution to engage both mesial frontal and orbital frontal cortex sources during the repeating cycles of spike–wave activity.

Conclusions: These data suggest that absence seizures are not truly “generalized,” with immediate global cortical involvement, but rather involve selective cortical networks, including orbital frontal and mesial frontal regions, in the propagation of ictal discharges. **Key Words:** Absence seizures—EEG—Source analysis—Dipole—Cerebral cortex—Thalamus.

The two major categories of epilepsy syndromes are referred to as localization-related or generalized (1). This dichotomous classification implies that seizures that originate from focal brain regions are associated with localization-related epilepsy; conversely, generalized epilepsy is characterized by seizures with diffuse, bilateral cerebral involvement. By definition, no evidence of structural brain lesions exists in persons with idiopathic generalized epilepsy.

The prototypic generalized seizure is the absence seizure, which may be present in several idiopathic generalized syndromes. The electroencephalographic (EEG) hallmark of absence consists of symmetric, bilateral, widespread spike–wave complexes, that, depending on the specific syndrome, range from 3 to 6 Hz and are commonly assumed to occur without lateralizing or localizing features (2). Experimental evidence that implicates thalamic and thalamocortical mechanisms as important in the

pathophysiology of absence may offer an explanation for the “generalized” nature of the ictus (3,4).

However, the “generalized” nature of absence seizures appears to be more a convention of interpretation rather than a description of the EEG evidence. Examination of EEG patterns in spike–wave discharges shows that, although they develop rapidly and may be difficult to lateralize, the spike–wave patterns are not diffuse but are predominant over the frontal cortex (5,6). This frontal distribution of both spikes and waves is clear in textbook examples of conventional EEG in absence seizures, even those that are described as having “generalized onset” (e.g., reference 6, p. 333). Other investigators pointed out that epileptiform discharges in some patients with childhood absence may appear “fragmentary,” especially during sleep, and produce focal spikes over centrotemporal and occipital regions (7). In some studies, spikes have been observed in conjunction with K-complexes during sleep onset (6). Whereas K-complexes are typically centered over the vertex in normal subjects, they appear more toward the frontal midline when associated with spikes in generalized epilepsy (6). This evidence of spike–wave seizures associated with activity in mesial frontal cortex

Accepted July 25, 2004.

Address correspondence and reprint requests to Dr. M.D. Holmes at Regional Epilepsy Center, Harborview Medical Center, Box 359745, 325 Ninth Avenue, Seattle, WA 98006, U.S.A. E-mail: mdholmes@u.washington.edu

during sleep onset may be congruent with the importance of corticothalamic circuitry in both spike-wave discharges and in sleep spindles in animal models (8).

With the advances in physical models of the neural sources of EEG activity in recent decades, it has become possible to relate the frontal distribution of spike-wave patterns to electrical sources in specific regions of frontal cortex. Applying equivalent dipole analysis to generalized spike-wave complexes with the spatiotemporal model has suggested that the most common model includes a source in the midline region of the basal frontal lobe (9). In further research, current source density analysis was applied to spike-wave patterns in conventional EEG recordings in five children with absence seizures (10). These analyses again emphasized the importance of inferior frontal generators, with spikes often showing a focal current distribution over frontopolar and orbital frontal cortex (10).

This evidence of a specific frontal cortical focus for generalized seizures may seem at variance with the evidence that thalamocortical mechanisms are responsible for widespread seizure discharges. However, neurophysiological analyses of thalamocortical augmenting and recruiting responses in animal experiments in the 1940s showed that cortical networks, specifically including orbital frontal cortex, were important in regulating the thalamocortical circuitry (11,12). With the modern recognition that this circuitry is mediated by the nucleus reticularis thalami (RE), the cortical modulation of thalamocortical controls by orbital frontal regions has been an important explanatory principle (13,14). The necessity of cortical involvement is clear in the corticothalamic circuitry of sleep spindles, also mediated by RE mechanisms and taken as a normal model for the circuitry that becomes pathological in spike-wave complexes (15,16). Furthermore, in an animal model of absence using intracranial EEG recordings, a cortical focus has been shown to drive spike-wave thalamocortical discharges, implying that the fundamental pathophysiology may, in fact, originate cortically (17).

With this background in mind, the present study was undertaken to explore the possibility that absence seizures in humans may involve activation of specific, rather than diffuse, cortical regions during ictal onset and propagation. To approach this problem, we recorded absence seizures with dense-array EEG recordings, a technique that improves the spatial resolution of scalp EEG (18). By implementing 256-channel recordings, we not only optimized spatial sampling but also achieved improved electrical sampling of the orbital, temporal, and occipital regions of the inferior brain surface (Fig. 1). By digitizing at 1,000 samples per second, we improved the temporal stability of the signal for examining scalp distributions and source models for the rapid transitions of the spike-wave complex. To examine the neural sources of the recorded scalp potentials, we applied two independent methods of EEG source analysis to the spike-wave

discharges of each seizure, equivalent dipole modeling (BESA), and low-resolution electromagnetic tomography (LORETA) (19–22). We examined the initial electrical activity of the seizure, as well as the stereotyped spike-wave pattern, to understand the onset of the pathological neurophysiologic activity as well as its typical propagation and cyclic pattern.

METHODS

Patients

Five patients with idiopathic generalized epilepsy composed this study. The epilepsy syndrome in all cases was established on the basis of history, age at onset, seizure types, clinical findings, standard EEG findings, and neuroimaging (2). All subjects underwent standard long-term video-EEG monitoring as part of an evaluation for difficult epilepsy, in which, in each instance, absence seizures were recorded and accompanied electrographically by generalized bursts of 3- to 6-Hz spike-slow wave or multiple spike-slow wave complexes. Subjects ranged in age from 18 to 58 years, and all were women. Both the clinical examinations and magnetic resonance imaging (MRI) studies were normal in every patient. None had any obvious risk factors for epilepsy except for a family history of epileptic seizures in one person.

Two subjects met criteria for typical childhood absence and manifested only absence seizures. Two had juvenile absence, with one having occasional generalized tonic-clonic convulsions in addition to frequent absences. The fifth subject had juvenile myoclonic epilepsy and, in addition to absence seizures, had daily myoclonic jerks and rare generalized tonic-clonic seizures.

Dense-array scalp EEG recordings

After approval by the University of Washington Human Subjects Review Committee, informed consent was obtained from each subject for ≤ 60 min of outpatient recordings with dense-array scalp EEG techniques. The 256-channel Geodesic Sensor Net was applied to each person during the recording (see Fig. 1), requiring ~ 10 min for application and adjustment. The EEG-amplifier characteristics included a bandpass of 0.1 to 400 Hz and sampling rate of 1,000 Hz, except in one case, in which the sampling rate was set at 500 Hz (with a 0.1- to 200-Hz bandpass). No effort was made to reduce or alter, for purposes of this study, any of the antiepileptic medications (AEDs) that each patient was routinely prescribed.

Spontaneous absence seizures were recorded in all instances, ranging in number from three to 11, depending on the subject. Every individual reported that she had experienced her usual absence seizures during the recording. The duration of spike-wave bursts varied from 3 to 40 s.

EEG referencing and mapping

The 256-channel EEG was recorded with a common vertex reference and rereferenced digitally to various

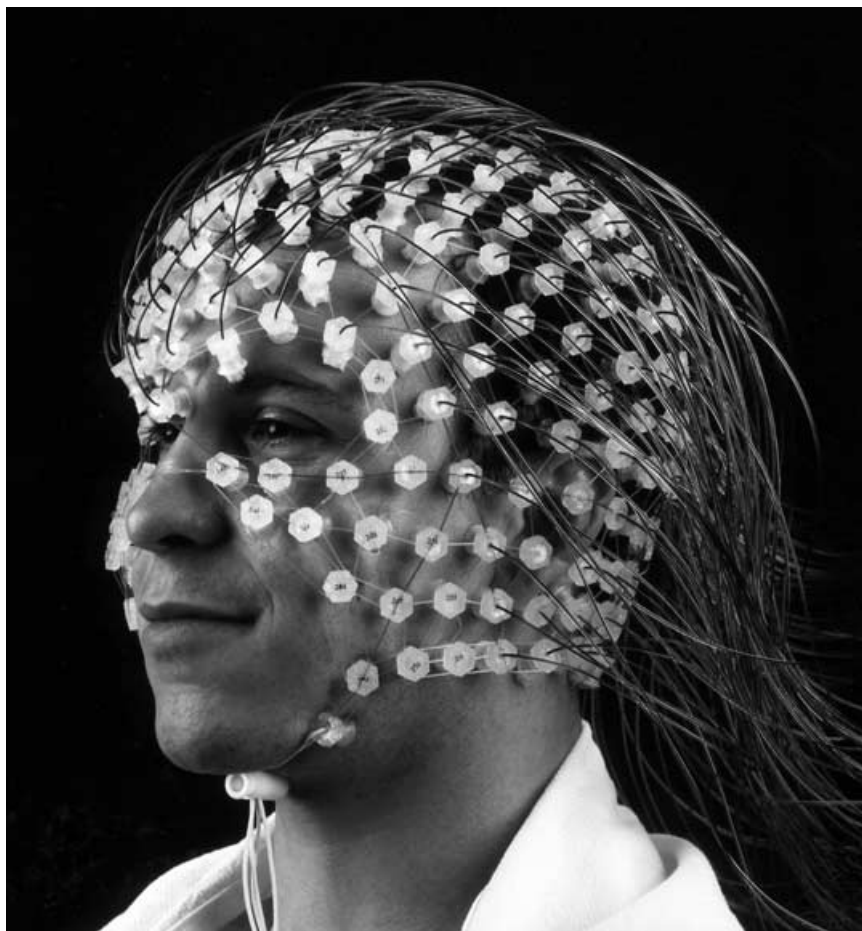


FIG. 1. 256-channel Geodesic Sensor Net[®] on a normal subject. The intersensor distance is about 2 cm on an average adult head. The improved coverage of the neck and face region allows improved reconstruction of cortical sources on the inferior surface of the brain.

montages for inspection, including the average reference. Because of the improved coverage of the inferior head surface of the 256-channel Geodesic Sensor Net, the average reference allows the potential at each index electrode to be examined with reference to an estimate of the zero potential of the head (23–26). The average-referenced EEG waveforms were examined with topographic waveform plots (e.g., Fig. 3), a technique that allows inspection of the geometric distribution of the potential fields. In addition, topographic maps were created with spherical spline interpolation (27). To examine the dynamic scalp topography of the spike–wave patterns, animations were created from maps interpolated at each 1-ms interval (28).

EEG source analysis

Two independent methods of source analysis were applied to the data. The first method was dipole modeling of the spike components of each spike–wave complex of each seizure, by use of brain electrical source activity (BESA) software (19,20). Although the spikes were the primary emphasis, separate dipole models were fit for the wave components. The data from all 256-channel recordings were used in the calculations. The dipole location, orien-

tation, and amplitude were estimated. We specified an ellipsoidal head model with four homogeneous shells: brain, CSF, skull, and scalp. Conductivity ratios were 1 (CSF), 0.3300 (brain), 0.0042 (skull), and 0.3300 (scalp). Thicknesses were 1 mm (CSF), 7 mm (skull), and 6 mm (scalp). Head radius was set to 92.5 mm (21).

Goodness-of-fit was estimated by residual variance, defined as the percentage of the spike variance that could not be explained by the model. For standardization, the residual variance was calculated at the midpoint of the rising slope of each spike. For purposes of illustration, we selected regional sources (with dipole moments in three orthogonal directions of space) that were most adequate to describe the entire spike–wave complex in its stereotyped form. Dipole locations were visualized in relation to a standard brain MRI model. Standard model MRIs were used in all source analyses instead of the subjects' own MRI, because the clinical MRIs were not “whole head” studies and were thus suboptimal in constructing volume conduction models. The positions of the electrodes with respect to the standard MRI models were determined by fitting actual 256-channel Geodesic Sensor Net locations to the sphere or ellipsoid approximation used in the source-localization

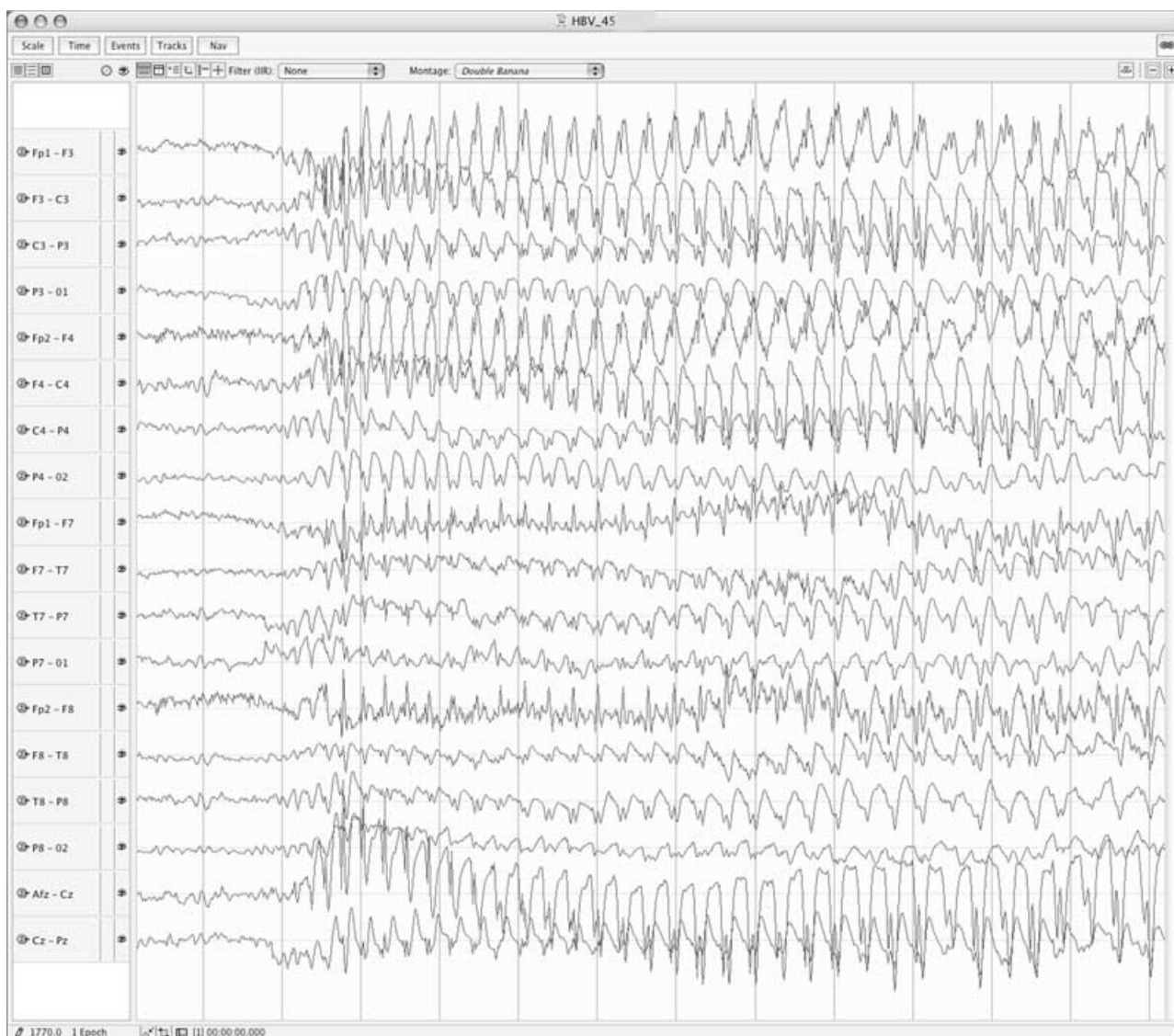


FIG. 2. Standard 10-20 montage for a seizure from one of the patients with childhood absence. Vertical lines at one second; simulated paper speed at 30 mm/sec, 0.1 to 400 Hz bandpass.

software. These locations were the average cartesian coordinates of the digitized locations from five normal adult subjects.

For an independent estimate of electrical sources, estimates of the three-dimensional cortical distributions of current source density of spikes and waves in each burst were accomplished by means of LORETA (22). This algorithm solves the inverse problem, assuming related orientations and strengths of neighboring neuronal sources, without assuming a specified number of sources. Mathematically, this is solved by finding the “smoothest” of all possible activity distributions. Although this assumption of a smooth distribution of electrical activity is useful for achieving a stable source localization, it should be emphasized that actual brain sources may have a more discrete distribution, such that the LORETA solution would then fail to reproduce the discrete localization accurately.

LORETA is registered to the Talairach Brain Atlas (29) and computes, at each voxel of the probabilistic cortical location, the current density as the linear weighted sum of the scalp electrical potentials. LORETA solutions were based on individual spikes within each spike-wave burst.

In addition to characterizing the spike and the wave features of the stereotyped cycles of the absence seizures, we also conducted dipole analysis and LORETA analysis of the EEG in the few seconds before seizure onset, to explore the possibly abnormal brain activity leading up to the seizure. For both methods of source analysis, the localization of results is only approximate in relation to brain structures, given that the EEG sensors were registered not to the patient’s individual MRI, but the typical locations of 256-channel Geodesic Sensor Net placement on an average head, using an average MRI for visualization.

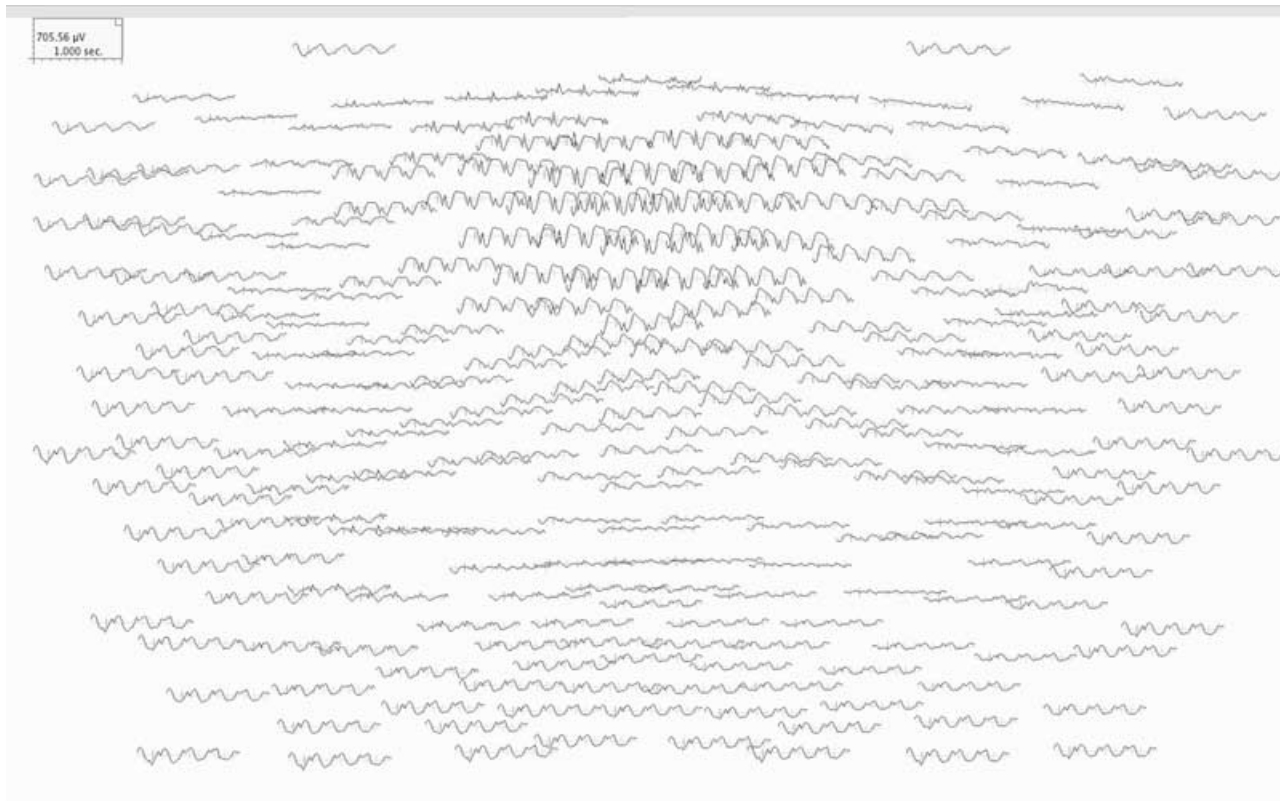


FIG. 3. Topographic waveform plot of 256 channels for the fourth second from Figure 2. Common Average reference (each channel is re-referenced to the mean of all channels). The view is looking down on the top of the head with the nose at the top of the page. A 1200 ms epoch is plotted for each of the 256 channels, in a schematic (topographic) arrangement of the position of the index electrode on the head. The spike-wave pattern is localized to the medial frontal sites.

RESULTS

Ictal onsets

The source solutions obtained by using equivalent dipole and LORETA methods yielded generally similar results for all seizures in regard to anatomic locations of ictal onsets and propagation over time. The fine details of the spatiotemporal evolution of each seizure could be discerned with either method, although somewhat more easily and more comprehensively with LORETA. Conversely, relating the temporal waveforms of source activity to the scalp EEG waveforms was easier with the equivalent dipole solutions, given that only a few dipoles were required for a reasonable model of the spikes and waves, whereas LORETA gives activations over a large number of source voxels. Seizure onsets showed variability in location from one subject to the next, and for any one patient, some degree of variability also was observed in regard to onsets. As was reported previously, slow, direct-current (DC) transitions are observed during the onset of each seizure that are not visible with a 1-Hz high-pass setting (5,6), and that would require DC amplification for accurate analysis (30).

For all seizures in all patients, ictal onsets, as defined by analysis of the first large-voltage transition before a spike-wave burst pattern, were found in discrete focal regions of

frontal lobe, affecting one side or the other. Frontal cortical regions most commonly involved include dorsolateral, orbital, or mesial frontal (cingulum). More than one region could be initially activated. Occasionally, simultaneous initial activation of focal regions of temporal or parietal lobe occurred during some seizures. The most consistent initial region of involvement was orbitofrontal cortex. Patterns of ictal onsets and propagation were similar in all patients, although number of subjects was too small to determine any differences based on specific epilepsy syndrome.

Ictal propagation

Regardless of the preictal transitions, the seizures in these five patients demonstrated a consistent, stereotyped pattern of propagation. An anterior negative slow wave was terminated by an abrupt spike transition that was focal over mesial frontopolar cortex. Because the slow wave precedes the first major spike (e.g., Figs. 2, 3, 6, and 7), the pattern may be more appropriately described as a wave-spike than a spike-wave, at least for the patients examined here. By the second to fourth spike after onset of the epileptiform discharge (i.e., within 1 s of seizure onset), the discharge showed a stereotyped mesial and anterior localization, and source analysis demonstrated that the cortical regions most activated were mesial frontal and

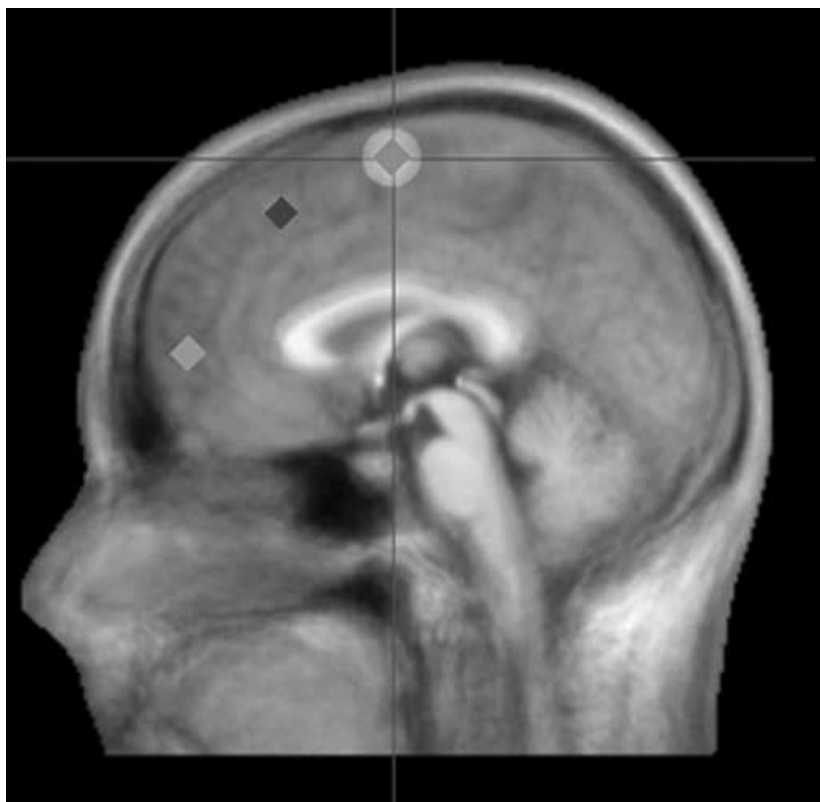


FIG. 4. Equivalent dipole source solutions for the spike-wave seizure from Figure 2, modeled in BESA, illustrated in approximate positions on an average MRI of an adult head. Each of the diamonds notes the location of a regional source (with dipole moments in x , y , and z orientations). With differing strengths for the three moments, the regional source is equivalent to a single dipole with a fixed orientation. Together, these sources provided an adequate model for the stereotyped spike-wave (or wave-spike) progression in Figure 2.

orbitofrontal regions. Although unique patterns of wave-spike complexes were observed for each patient (see examples in Figs. 2 and 6), a common pattern was a negative anterior slow wave, an abrupt negative spike in

orbitofrontal cortex (which may produce a positive field distribution over some regions of the dorsolateral frontal lobe in some cases), and then an abrupt midline positive spike (with a mesial frontal localization) that may be

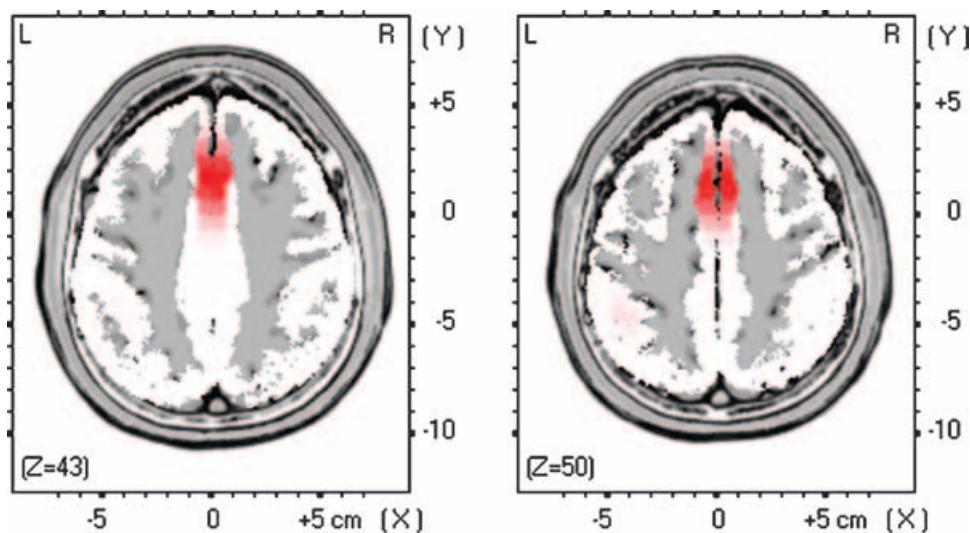


FIG. 5. Axial slices from the LORETA solution for the seizure from Figure 2, illustrated in relation to cortical gray matter on an average MRI. This slice shows the strongest source distribution for this time sample. At this level, LORETA is modeling the source in the anterior cingulate or supplementary motor area modeled as the posterior equivalent dipole in Figure 4. This source is particularly strong during the negative anterior slow wave. The source shown by the red source intensity maximum in these MRI slices is aligned approximately with the red regional source dipole in Figure 4.

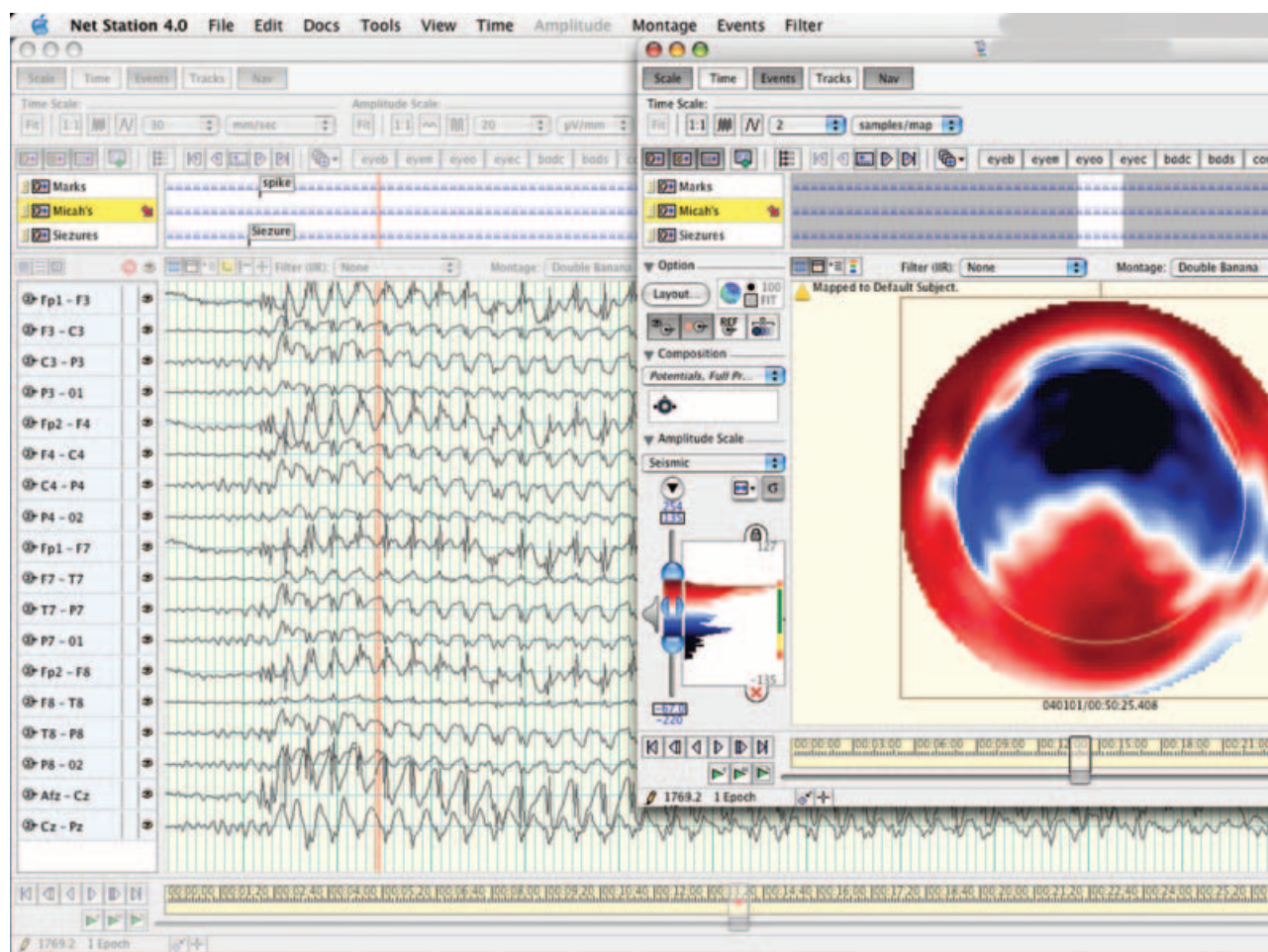


FIG. 6. Seizure from a subject with juvenile absence. The map is synchronized with the red vertical line in the chart view, aligned with the wave preceding the fifth complete wave-spike complex (time 50 minutes, 25 seconds, 408 milliseconds into the recording). The white circle in the map marks the canthomeatal line or approximate equator of the head. The color palette (shown in the histogram of amplitude values at the left of the map) displays negative potentials in blue and positive potentials in red, with white at the zero isopotential. The topographic map at this 408 ms sample shows the frontal negative (and posterior positive) distribution typical of anterior negative slow waves.

associated with additional positive features, depending on the individual patient. Finally, the cycle repeats with the next negative anterior slow wave.

Although these general features were observed in all five cases, specific patterns were seen for individual patients. Figure 2 shows a conventional bipolar montage of 10-20 channels for a wave-spike discharge during an absence seizure in a patient with childhood absence syndrome. This recording with 0.01-Hz high-pass (10-s time constant) illustrates the DC transitions that are typical in absence seizure onset (5) and that have been found to be localizing in temporal lobe seizure onset (30). Given the frontal polar distribution of the slow negative shifts in the absence seizures examined here, they may be localizing in these seizures as well, although true DC recordings are required for a confident interpretation of this issue. The wave-spike discharges in Figure 2 show the typical frontal distribution observed with conventional EEG with international 10-20 system locations (5,6).

The full 256-channel montage is shown for a 1-s segment of this discharge in Figure 3, in a topographic waveform plot with average reference. The need for dense-array spatial sampling is shown by the abrupt divergence between many adjacent electrodes. The focal distribution of the wave-spike pattern is clearly seen, and it is apparent that the wave and spike do not share the same topography. The anterior negative wave has a mesial and somewhat broad distribution, whereas the negative anterior spike extends to orbital frontopolar regions that show minimal slow wave.

The differentiation of the slow wave from frontopolar spike, and of both from interposed positive transitions and waves, was confirmed by their differential source modeling. Although substantial variability is apparent across patients in the specific source model (and scalp topography), the negative anterior slow wave and many positive spikes and waves often show localization to mesial frontal (anterior cingulate, supplementary motor area or SMA,

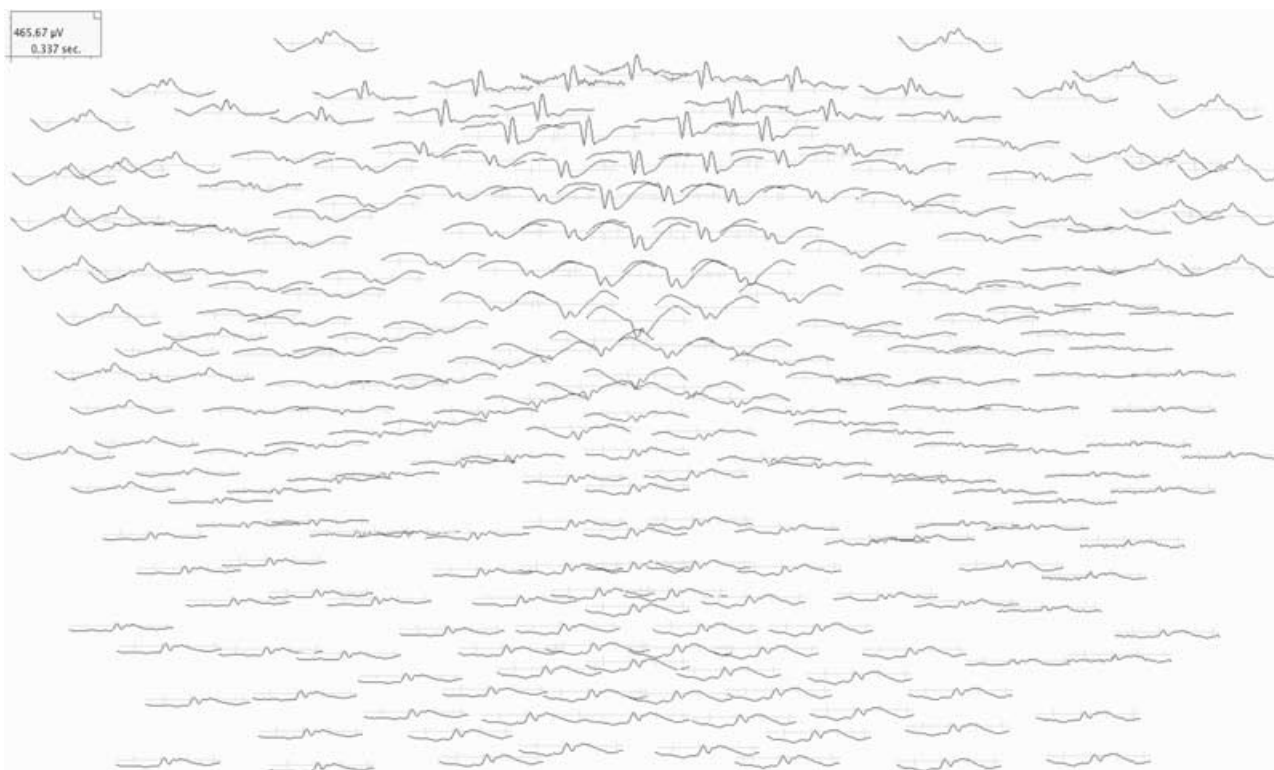


FIG. 7. Fifth wave-spike complex from the seizure in Figure 6, shown in average reference topographic waveform plot. The format is similar to Figure 3, except that the time axis for each epoch has been expanded so that 400 ms is displayed from each channel. As for the seizure shown in Figure 3, the spike-wave complex is localized primarily to the medial frontal region. However, for this seizure for this patient, there is some inversion of the spike-wave pattern to the posterior midline that was not seen for the data in Figure 3.

and more anterior midline) sources. In contrast, the negative frontopolar spike transition shows a consistent tendency to be modeled best by an orbital, frontopolar dipole source. Figure 4 shows the equivalent regional (three-moment) dipole model that characterized the stereotyped wave-spike pattern of the seizure in Fig. 2. In this and in many other absence wave-spike cycles, the negative anterior slow wave was modeled best not by the frontopolar source, but by the dorsomedial frontal sources, with strong moment strengths of the tangential (rostrocaudal) orientation, producing simultaneous anterior negative and posterior positive potential distributions. Figure 5 shows the LORETA solution for the negative slow wave for this discharge, with strong activation of the SMA or anterior cingulate source. A limitation of this LORETA implementation is that only the magnitude and not the orientation is displayed.

For another example, Figure 6 shows an absence seizure in a patient with juvenile absence syndrome. To illustrate the dynamic and focal topography of the wave-spike pattern, the topographic map is synchronized with the 10-20 montage at the anterior negative slow wave of the fifth wave-spike complex of this discharge (time 50:25.408), when the pattern has become fully stereotyped. The color palette shows negative potentials in blue, positive potentials in red, and the zero level (estimated by the average

reference) in white. This fifth wave-spike is shown in its entirety (337 ms) in Figure 7 in a topographic waveform plot. As with the previous patient, the wave and spike are both focal and anterior, but the negative anterior slow wave is more mesial and broadly distributed, whereas the frontopolar negative spike is strong over the lower forehead where the negative anterior slow wave is attenuated. The inversions of wave topography are useful in localizing the ictal event in this display as well. Although certain waveform features, such as the positive-going spike at the termination of the anterior negative slow wave, invert in a rostrocaudal direction along the midline (consistent with a tangential source in the mesial frontal lobe), other features, such as the negative anterior slow wave itself, seem to invert in a superior-inferior direction (shown mesial frontal to lateral frontal on this plot), suggesting a vertical orientation of the dominant source in this patient.

To illustrate the dynamics of the scalp topography more closely, topographic maps were created for selected time points for the wave-spike cycle in Figure 7 and are shown in Figure 8. The first map (ms 436) is just after that shown in Figure 6 and continues to show the negative anterior slow wave. Between 505 and 514 ms, the abrupt anterior transition of the termination of the slow wave is accompanied by a rapid shift of the positive midline potential toward the frontal pole. This produces the positive spike

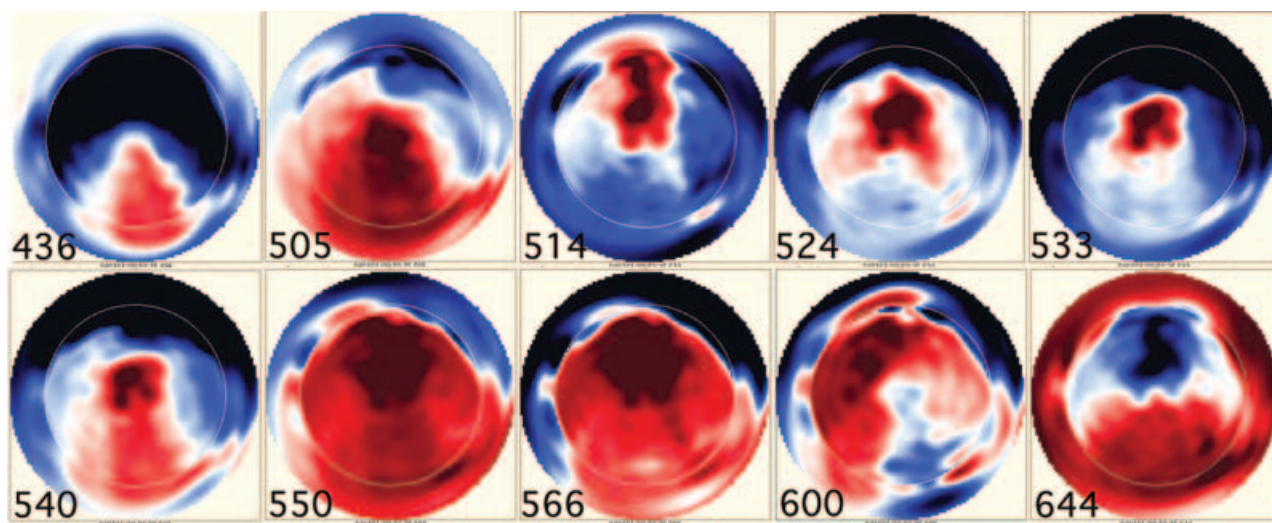


FIG. 8. Map series for fifth wave-spike complex from the seizure in Figure 6. Recording time 50 minutes, 25 seconds. Within this second, samples were selected to illustrate transitions in scalp topography. The top row shows milliseconds 436, 505, 514, 524, and 533. The bottom row shows milliseconds 540, 550, 566, 600, and 644. At 436 ms, the anterior-negative slow wave can be seen. After an abrupt spike transition at the midline frontal pole (505 ms), a positive spike appears to sweep from posterior midline toward anterior midline (514 ms). This positive midline spike shifts back to a focal central midline site (524-540 ms), and then increases in amplitude and extent to create a broad superior-frontal positive, inferior-frontal negative distribution (550-566 ms) for the second positive spike of this complex (as can be seen in the topographic wave plot of these data in Figure 7). As this second positive frontal spike resolves (600 ms), it is replaced by the onset of the anterior-negative slow wave of the next spike-wave complex (644 ms).

terminating the anterior negative slow wave in Figure 7. In the LORETA solution computed for each millisecond and animated over time, this transition appears as a sweep of activity from the dorsal anterior cingulate along the mesial surfaces of the frontal lobes toward the frontal pole. At ms 524 and 533, the frontopolar negative spike replaces the positive mesial frontal spike, and, as it resolves by 540 ms, it is replaced by a broad frontal positive wave (550). This wave in turn resolves slowly (566 and 600) until it is replaced by the anterior negative slow wave (644) of the next wave-spike cycle.

The equivalent dipole model for this cycle of events is shown in Figure 9. As is typical for these five patients, three sources provided an approximate summary of the wave-spike pattern once it became stereotyped. Although some periods of superposition are confusing, the time dynamics of the activation of these sources can generally be inferred from the progression of the surface topography in Figure 8. Figure 10 shows the LORETA solution for the 514-ms time point in Figure 8. Whereas the mid-cingulate/SMA activation of the negative anterior slow wave remains strong, a new activation sweeps along the mesial surface of the dorsal frontal lobe toward the frontal pole, corresponding to the midline forward shift of the positive spike transition at 514 ms in Figure 8.

DISCUSSION

The hypothesis that the spike-wave discharges observed in absence and other forms of generalized seizures are mediated through thalamic and thalamocortical (TC) circuits is several decades old (31). Research since then

has reinforced the notion that TC circuits are involved in normal and abnormal cerebral rhythmicity and are thereby of major importance in the pathophysiology of generalized epilepsy (3). Investigators report that spike-wave discharges may result from an aberration of the same TC circuits that modulate physiologic sleep spindles (15,16). Other lines of research implicate thalamic T-type voltage-gated calcium channels in the pathogenesis of absence epilepsy (32,33), whereas studies that involve proton magnetic resonance spectroscopy (MRS) demonstrate abnormal ratios of *N*-acetylaspartate and creatine-phosphocreatine in the thalami of individuals with some forms of primary generalized seizures compared with those in controls (34). The research that identifies the importance of thalamic and TC mechanisms in the formation of spike-wave discharges forms the basis of an explanation for the apparently diffuse and bilaterally synchronous nature of a generalized seizure, both at onset and during propagation of the ictus.

However, despite abundant evidence of an important role for subcortical mechanisms in generalized epilepsy, it also is clear that the cerebral cortex plays a critical, and perhaps fundamental, role in the pathophysiology of these seizures. In a study of a rat model of absence that used intracranial EEG recordings, not only was cortical focality observed during spontaneous seizures, but it was the cortical focus that drove the TC circuits during the seizure, and not the other way around (17). A crucial role of the cerebral cortex in the pathogenesis of generalized epilepsy is the implication of other data that show that cortical excitability is enhanced in patients with some forms

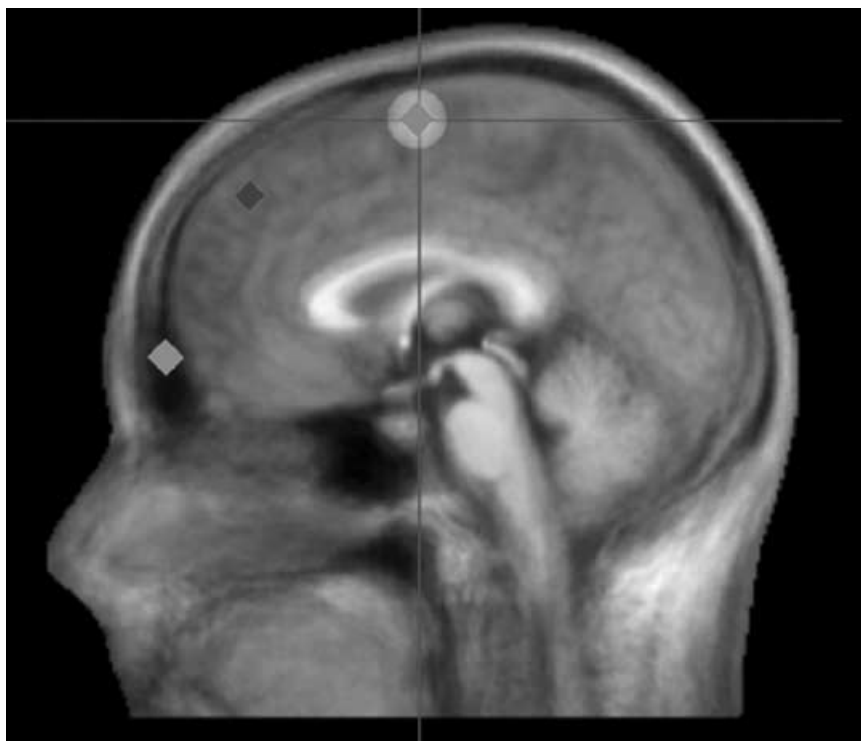


FIG. 9. Equivalent dipole source model for the ictal onset and progression of the seizure from Figure 6. Each of the diamonds notes the location of a regional source (with dipole moments in x, y, and z orientations). Together, these sources provided an adequate model for the stereotyped spike-wave progression shown in Figure 6.

of primary generalized epilepsy (35). Animal studies have shown that targeting thalamic nuclei is insufficient for the full antiabsence effect of ethosuximide (ESM), suggesting that the antiabsence action of this agent may reside exclusively, or least primarily, in the cortex (36).

The likely focal cortical nature of generalized epilepsy may have an anatomic basis. Foci of cortical microdysgenesis have been reported in pathological studies of individuals who had primary generalized epilepsy in life (37). MRI studies suggest cortical abnormalities in mesial frontal cortex of subjects with juvenile myoclonic epilepsy (38), whereas proton MRS investigations disclose regional metabolic abnormalities in frontal (39) and occipital (40) lobes in patients with generalized epilepsy syndromes.

The present results confirm the importance of frontopolar activity in absence seizures suggested by source analysis of conventional EEG (9,10). With dense-array EEG recording, the focal topography of the wave-and-spike morphology of the absence seizure is apparent from visual inspection of the scalp potential distributions, although both distributed (LORETA) and point dipole (BESA) models were useful in confirming the importance of a frontopolar source to the spike-transition event that appeared in most seizures interposed with the anterior negative slow wave. Future research that uses more advanced source-analysis techniques and estimates of time delays between relevant sources will be important in achieving

greater insight into underlying processes and propagation pathways.

The specificity of orbital and frontopolar control over thalamic regulatory mechanisms has been apparent since the early neurophysiologic studies of frontothalamic augmenting responses (11,12). In analyzing the frontothalamic circuitry common to both spike-wave seizures and sleep spindles, research has shown that the cyclic nature of these neurophysiologic rhythms can be traced to membrane properties of thalamocortical neurons, including low-threshold spikes and calcium conductance mechanisms that appear to be targeted by ESM (36). However, thalamic circuits are not entirely diffuse in their activity, but are themselves regulated by frontothalamic circuits, including the orbital frontal cortex specifically. The thalamocortical neurons are inhibited by the nucleus reticularis thalami (RE), which is in turn inhibited by orbital frontal cortex (13,14). Consistent with this circuitry, frontothalamic augmenting responses in animal studies are not only elicited by electrical stimulation of orbital frontal cortex, but they also are abolished specifically by lesions of orbital cortex and not by other lesions of the frontal lobe (11,12).

In addition to frontopolar sources, electrical discharges in the present series of subjects also were localized to the cingulate gyrus and associated neocortex in the mesial frontal lobe. Activity in these regions was important not only to the anterior negative slow wave of the wave-spike

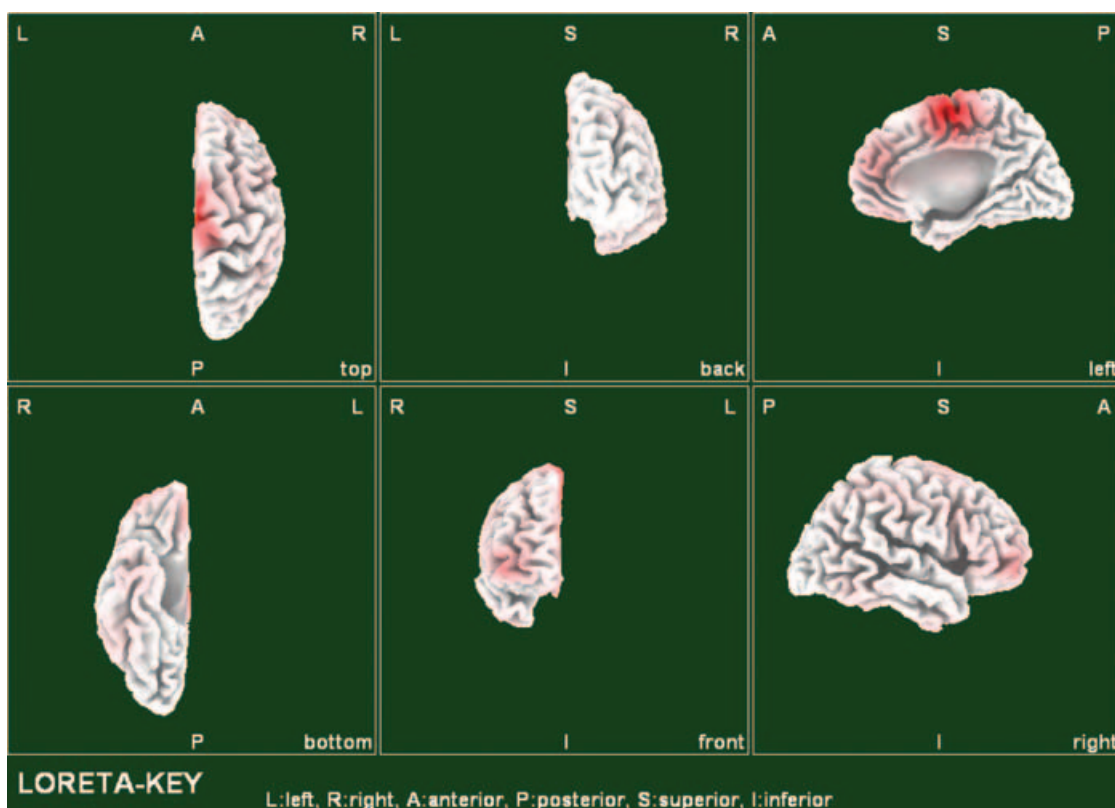


FIG. 10. LORETA solution for 514 ms time sample mapped in Figure 8, projected to the cortical surface from a typical adult MRI. This distributed source model suggests that the primary neural activity contributing to the first midline positive spike of this spike-wave complex is localized initially in the medial walls of the hemispheres (shown here for the right hemisphere), in the general region of the supplementary motor area and cingulate cortex.

discharge, but also to the positive spikes that were integral to the rapid transitions of ictal events in the frontal lobe, including the remarkable sweep of surface-positive activity from the cingulate toward the frontal pole at the termination of the anterior negative slow wave that was a common event in our patients (e.g., Fig. 8, ms 505–514).

Further research is required to understand the significance of this mesial frontal activity to the frontothalamic dysregulation in absence seizures. The anterior cingulate cortex (ACC) is critical to self-regulation of frontothalamic circuits (41,42) and to maintenance of arousal in both animal and human studies (43–45). The integral role of ACC and midcingulate activity in the present data may be consistent with the importance of mesial frontal networks in both arousal control and generalized epilepsy (6).

This study demonstrates that absence seizures are not “generalized” in the sense of homogeneous cortical activation but involve highly localized discharges from mesial frontal and frontopolar sources. Whether the concern is with genetic mechanisms of risk or pharmacologic interventions for modifying neural excitability, it will be important in both research and clinical practice to parallel the increasing specificity in molecular neuroscience with increasing specificity in the measurement of pathologic neurophysiological activity.

REFERENCES

1. Commission on Classification and Terminology of the International League Against Epilepsy. Proposal for revised classification of epilepsies and epileptic syndromes. *Epilepsia* 1989;30:389–99.
2. Panayiotopoulos C. Idiopathic generalized epilepsies. In: Panayiotopoulos C, ed. *A clinical guide to epileptic syndromes and their treatment*. Oxfordshire, UK: Bladen Medical Publishing, 2002:114–60.
3. McCormick D. Cortical and subcortical generators of normal and abnormal rhythmicity. *Int Rev Neurobiol* 2002;49:99–114.
4. Slaght S, Leresche N, Denian J, et al. Activity of thalamic reticular neurons during spontaneous genetically determined spike and wave discharges. *J Neurosci* 2002;22:2323–34.
5. Goldensohn E, Legatt A, Koszer S, Wolf S. *Goldensohn's EEG interpretation: problems of overreading and underreading*. Armonk, NY: Futura, 1999.
6. Niedermeyer E. Epileptic seizure disorders. In: Niedermeyer E, Lopes da Silva F, eds. *Electroencephalography: basic principles, clinical applications, and related fields*. Baltimore: Urban & Schwarzenberg, 2000:476–585.
7. Panayiotopoulos C. The clinical spectrum of typical absence seizures and absence epilepsies. In: Malafosse A, Genton P, Hirsch E, et al., eds. *Idiopathic generalized epilepsies*. London: John Libbey, 1994:75–85.
8. Steriade M, Amzica F. Sleep oscillations developing into seizures on corticothalamic systems. *Epilepsia* 2003;44(suppl 12):9–20.
9. Rodin E, Rodin M, Thompson J. Source analysis of generalized spike-wave complexes. *Brain Topogr* 1994;7:113–9.
10. Rodin E. Decomposition and mapping of generalized spike-wave complexes. *Clin Neurophysiol* 1999;110:1868–75.
11. Morrison R, Dempsey E. A study of thalamocortical relations. *Am J Physiol* 1942;135:281–92.

12. Morrison R, Dempsey E. Mechanism of thalamocortical augmentation and repetition. *Am J Physiol* 1943;138:297–308.
13. Yingling C, Skinner J. Selective regulation of thalamic sensory relay nuclei by nucleus reticularis thalami. *Electroencephalogr Clin Neurophysiol* 1976;41:476–82.
14. Yingling C, Skinner J. Gating of thalamic input to cerebral cortex by nucleus reticularis thalami. In Desmedt JE, ed. *Attention voluntary contraction and event-related cerebral potentials: progress in clinical neurophysiology*. Vol I. Basel: Karger, 1977:70–96.
15. Steriade M. *Neuronal substrates of sleep and epilepsy*. New York: Cambridge University Press, 2003.
16. Steriade M, Amzica F. Sleep oscillations developing into seizures in corticothalamic systems. *Epilepsia* 2003;44(suppl 12):9–20.
17. Meeren H, Pijn J, Van Luijckelaar E, et al. Cortical focus drives widespread corticothalamic networks during spontaneous absence seizures in rats. *J Neurosci* 2002;22:1480–95.
18. Lantz G, Grave de Peralta R, Spinelli L, et al. Epileptic source localization with high density EEG: How many electrodes are needed? *Clin Neurophysiol* 2003;114:63–9.
19. Scherg M, Ebersole J. Brain source imaging of focal and multifocal epileptiform EEG activity. *Clin Neurophysiol* 1994;24:51–60.
20. Scherg M, Ille N, Bornfleth H, et al. Advanced tools for digital EEG review: virtual source montages, whole-head mapping, correlation, and phase analysis. *J Clin Neurophysiol* 2002;19:91–112.
21. Berg P, Scherg M. A fast method for forward computation of multiple-shell spherical head models. *Electroencephalogr Clin Neurophysiol* 1994;90:58–64.
22. Pasqual-Marqui R, Essen M, Kochi K, et al. Functional imaging with low-resolution brain electromagnetic tomography (LORETA): a review. *Methods Find Exp Clin Pharmacol* 2002;24(suppl C):91–5.
23. Phillips C, Rugg M, Friston K. Anatomically informed basis functions for EEG source localization: combining functional and anatomic constraints. *Neuroimage* 2002;16:678–95.
24. Bertrand O, Perrin F, Pernier J. A theoretical justification of the average-reference in topographic evoked potential studies. *Electroencephalogr Clin Neurophysiol* 1985;62:462–4.
25. Dien J. Issues in the application of the average reference: review, critiques, and recommendations. *Behav Res Method Instrum Comput* 1998;30:34–43.
26. Junghofer M, Elbert T, Tucker D, et al. The polar average reference effect: a bias in estimating the head surface integral in EEG recording. *Clin Neurophysiol* 1999;110:1149–55.
27. Perrin F, Pernier J, Bertrand O, et al. Mapping of scalp potentials by surface spline interpolation. *Electroencephalogr Clin Neurophysiol* 1987;66:75–81.
28. Tucker D, Liotti M, Potts G, et al. Spatiotemporal analysis of brain electrical fields. *Hum Brain Mapp* 1994;1:134–52.
29. Talairach J, Tournoux P. *Co-planar stereotactic atlas of the human brain*. Stuttgart: Thieme, 1988.
30. Vanhatalo S, Holmes M, Tallgren P, et al. Very slow EEG responses lateralize temporal lobe seizures: an evaluation of non-invasive DC-EEG. *Neurology* 2003;60:1098–104.
31. Gloor P. Generalized epilepsy with bilateral synchronous spike and discharge: new findings concerning its physiological mechanisms. *Electroencephalogr Clin Neurophysiol Suppl* 1978;34:245–9.
32. Huguenard J. Neuronal circuitry of thalamocortical epilepsy and mechanisms of antiabsence drug action. *Adv Neurol* 1999;79:991–9.
33. Kim D, Song I, Keum T, et al. Lack of the burst firing of thalamocortical relay neurons and resistance to absence seizures in mice lacking the $\alpha 10$ T-type Ca^{++} channels. *Neuron* 2001;31:35–45.
34. Mory S, Li L, Guerreiro C, et al. Thalamic dysfunction in juvenile myoclonic epilepsy. *Epilepsia* 2003;44:1402–5.
35. Brodtmann A, Macdonnell R, Gilligan A, et al. Cortical excitability and recovery curve analysis in generalized epilepsy. *Neurology* 1999;53:1347–9.
36. Richards, D, Manning J, Barnes D, et al. Targeting thalamic nuclei is not sufficient for the full anti-absence action of ethosuximide in a rat model of absence epilepsy. *Epilepsy Res* 2003;54:97–107.
37. Meencke H, Janz D. Neuropathological findings in primary generalized epilepsy: a study of eight cases. *Epilepsia* 1984;25:8–21.
38. Woermann F, Free S, Koepp M, et al. Abnormal cerebral structure in juvenile myoclonic epilepsy demonstrated with voxel-based analysis of MRI. *Brain* 1999;122:2101–7.
39. Simister R, McLean M, Barker G, et al. Proton MRS reveals frontal lobe metabolic abnormalities in idiopathic generalized epilepsy. *Neurology* 2003;61:897–902.
40. Simister R, McLean M, Barker G, et al. A proton magnetic resonance imaging spectroscopy study of metabolites in the occipital lobes in epilepsy. *Epilepsia* 2003;44:550–8.
41. Gabriel M. Functions of anterior and posterior cingulate cortex during avoidance learning in rabbits. *Progr Brain Res* 1990;85:467–83.
42. Vogt B, Finch D, Olson C. Functional heterogeneity in the cingulate cortex: the anterior executive and posterior evaluative regions. *Cereb Cortex* 1993;2:435–43.
43. Paus T. Functional anatomy of arousal and attention systems in the human brain. *Progr Brain Res* 2000;126:65–77.
44. Luu P, Flaisch T, Tucker D. Medial frontal cortex in action monitoring. *J Neurosci* 2000;20:464–9.
45. Luu P, Tucker D. Self-regulation and the executive functions: electrophysiological clues. In: Zani A, Preverbio A, eds. *The cognitive electrophysiology of mind and brain*. San Diego: Academic Press, 2003:199–223.